Toroidal Rotation Profiles under the Influence of Fast-ion Losses Due to Toroidal Field Ripple

Mitsuru HONDA, Tomonori TAKIZUKA, Atsushi FUKUYAMA[1)], Maiko YOSHIDA and Takahisa OZEKI

Japan Atomic Energy Agency, Naka, Ibaraki 311-0193, Japan
[1)]*Graduate School of Engineering, Kyoto University, Sakyo, Kyoto 606-8501, Japan*

Characteristics of toroidal rotation profiles in tokamak plasmas are studied under the influence of fast-ion losses due to a toroidal field (TF) ripple by using a one-dimensional multi-fluid transport code, TASK/TX. When a neutral beam (NB) is injected into a plasma, a part of fast ions is lost due to the effect of the TF ripple. The radial current then flows inward in the bulk plasma to keep quasi-neutrality and it exerts a torque on the plasma in the direction opposite to the plasma current. A parametric survey of the toroidal rotation driven by this torque is conducted to quantify the sensitivity to various externally-controllable sources such as a co-tangential NBI power. In the case of a larger ripple amplitude, it is observed that the counter-toroidal rotation develops near the periphery of the plasma as an increase in the co-NBI input power while the co-toroidal rotation velocity on the magnetic axis reaches a maximum value at a certain NBI power. This torque can be mitigated by increasing a gas puff rate. An increase in the plasma current also leads to the reduction in the counter rotation induced by ripple.

Keywords: toroidal rotation, toroidal field ripple, fast-ion loss, transport simulation, tokamak

1. Introduction

In recent years, the toroidal rotation has been brought to attention in a tokamak field because it is commonly believed that the rotation plays an essential role in the formation of internal transport barriers, the L-H transition, the suppression of resistive wall modes and so forth. It is important to acquire a capability of predicting and controlling the toroidal rotation in present tokamaks, particularly ITER and future reactors. The physics of momentum transport governing the toroidal rotation has been therefore studied both theoretically and experimentally.

The tangentially-injected NB is the most useful instrument to drive the plasma rotation: fast ions generated in the plasma run along the field line and they gradually transfer their momentum to the bulk plasma through the collisional slowing-down process. However, it has been reported from the experiments on JT-60U [1] and JET [2] that the counter rotation is observed near the peripheral region despite tangential co-NBs. The features of the rotation in JT-60U were altered after the insertion of ferritic steel tiles (FSTs) in a vacuum vessel, which reduces a toroidal field ripple almost by half [1]. The experimental observation implies the strong linkage between the loss of fast ions and the reversal of the direction of the toroidal rotation near the periphery.

In our recent work [3], we have qualitatively reproduced the tendency of toroidal rotation profiles observed in the JT-60U experiments with and without FSTs as shown in Fig. 1, by numerical simulations with the TASK/TX code. The TASK/TX simulations clearly show that the loss of fast beam ions due to ripple induces the inward radial current in the bulk plasma to maintain quasi-neutrality and a resultant $j \times B$ torque overcomes a collisional di-
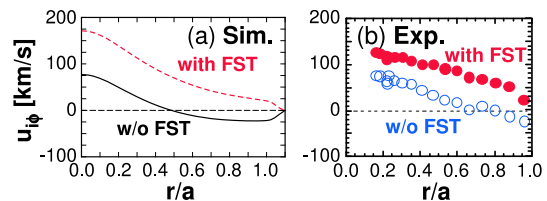

Fig. 1 Toroidal rotation profiles under the influence of ripple in (a) simulations and (b) JT-60U experiments [3].

rect torque from co-NBIs near the periphery, inducing the counter rotation, when the ripple amplitude is sufficiently large, i.e. the case without FSTs. Based on this understanding of the physical mechanism, in this paper we study the behavior of the toroidal rotation under the influence of the TF ripple when we vary a NBI input power, a gas puff rate and a plasma current, by utilizing the TASK/TX code with the newly-developed ripple transport model. This may give us insights into the toroidal rotation.

2. Transport modelling
2.1 Multi-fluid transport code, TASK/TX

Here we summarize the main characteristics of the one-dimensional multi-fluid transport code TASK/TX with an emphasis on the difference from conventional transport codes, and one can see more details about the code in [4].

- The code solves the continuity equations, the thermal transport equations and the two-fluid equations of motion for electrons and ions coupled with Maxwell's equations as well as the equations for neutrals and fast beam ions in the cylindrical coordinates (r, θ, ϕ), where r, θ and ϕ denote the radial, poloidal and

author's e-mail: honda.mitsuru@jaea.go.jp

toroidal directions respectively .

- Since the multiple continuity equations for all charged particle species and Poisson's equation are simultaneously solved, an explicit quasi-neutrality condition is not imposed on the code.
- Neoclassical effects such as the bootstrap current and the Ware pinch are described through the parallel viscous force term in the equation of motion in the poloidal direction.
- Turbulent ambipolar transport is expressed by the poloidal momentum exchange between electrons and ions; hence an explicit particle diffusivity need not be added in the continuity equations.
- In order to investigate a structure of a plasma near the plasma surface (separatrix), the code takes into account the transport in the scrape off layer.
- The formation of the radial electric field is accurately evaluated in a manner consistent with the flows.

Above all, the feature that there is no need to impose an explicit quasi-neutrality condition, which notably distinguishes the code from other transport codes, is essential to this study. This is because we examine how a violation of quasi-neutrality due to a non-ambipolar loss of fast ions due to ripple provokes the $j \times B$ torque in the bulk plasma and then how the resultant rotation is in a quasi-steady state. In the next subsection, we briefly discuss a transport modelling of fast-ion losses due to ripple used in the code.

2.2 Ripple transport model for fast ions

The finite number of TF coils of an actual tokamak destroys the ideal toroidal symmetry and these coils produce a TF ripple with a three-dimensional structure. Focusing on the enhancement of the transport for fast ions induced by this TF ripple, we have developed and introduced a ripple transport model suitable for a fluid-type transport code.

In the presence of the ripple magnetic field, there exist local magnetic wells where the following condition is satisfied [5]:

$$\alpha(r, \theta) \equiv \frac{\epsilon |\sin \theta|}{N q \delta} < 1. \qquad (1)$$

Here ϵ denotes the inverse aspect ratio, θ the poloidal angle, N the number of TF coils, q the safety factor and δ the ripple amplitude. The region usually covers a large amount of the lower-field side of the poloidal cross-section. Since a ripple magnetic well acts just like a neoclassical magnetic mirror, the ripple mirror can potentially trap a fast ion with a small parallel velocity. Therefore fast ions residing in the ripple well region are trapped when they are in the trapped velocity band: $|v_{\parallel}/v| < \sqrt{\delta}$. If the ions are captured in the local ripple mirrors, they cannot move freely along the field line. We then separate the beam ions into two categories: the ripple-untrapped ions and the ripple-trapped ones, because the latter cannot directly carry their

momentum along the field line as is pointed out above. The ripple-trapped ions mainly suffer from the ∇B drift This is a very rapid process compared with a diffusive process from which they also suffer.

Unlike the convective loss process for the ripple-trapped ions, the diffusive process is dominant for ripple-untrapped banana ions. When the banana ions are in the ripple well region, they suffer from the diffusion due to ripple only at the banana tips where their parallel velocity becomes zero. We assume that the diffusive process consists of two major processes: the collisional diffusion and the collisionless stochastic diffusion, and furthermore the former consists of the ripple-plateau diffusion and the ripple-banana diffusion from the aspect of the collisionality. The main diffusive loss channel for the banana ions is the collisionless stochastic diffusion, which occurs in the localized region only where the local ripple amplitude exceeds the Goldston-White-Boozer (GWB) criterion δ_{GWB} [6], typically near the periphery. Finally, the trajectory of ripple-untrapped passing particles is hardly disturbed by a TF ripple because of their rapid velocity, and thus the effect of the ripple on them is negligible.

In our ripple model, a near-perpendicular NBI and a collisional deflection process are the main sources of the ripple-trapped beam ions. The banana ions near the ripple-trapped velocity band in the velocity space can easily enter the velocity band through collisional scattering and they turn out to be the ripple-trapped ones. The opposite process also occurs. This source of the ripple-trapped ions through deflection collisions can be described as

$$S_b^{def} = \frac{\nu_D}{\delta} (\sqrt{\delta} n_b - n_b^{rp}), \qquad (2)$$

where ν_D denotes the deflection rate which measures the average rate at which the particle velocity is scattered into the direction perpendicular to its initial velocity, n_b and n_b^{rp} the densities for the ripple-untrapped and ripple-trapped ions, respectively. For more details about the ripple transport model, see [3].

3. Dependence on the NBI input power

In the following, we apply the JT-60U-like parameters without FSTs used in section 4.1 of [3] as the reference case. Typical parameters are: the major radius $R_0 = 3.4$ m, the minor radius $a = 0.95$ m, the toroidal magnetic field $B_{\phi} = 2.6$ T, the plasma current $I_p = 1.0$ MA, the safety factor at the 95% flux surface $q_{95} = 3.3$, the gas puff rate $\Gamma_0 = 0.2 \times 10^{20}$ m^{-2}s^{-1}, the input powers of the co-tangential NBIs and the near-perpendicular NBI $P_{co} = 3.2$ MW and $P_{perp} = 0.4$ MW. A peak of the deposition profile of the co-tangential NBI is located close to the magnetic axis. In this configuration without FSTs, the ripple amplitude at the plasma surface is $\delta_a = 1.28\%$ in the equatorial plane. In the case with FSTs, we reduce the ripple amplitude by half, $\delta_a = 0.64\%$, according to the experimental observation [1]. In our study, turbulent vis-
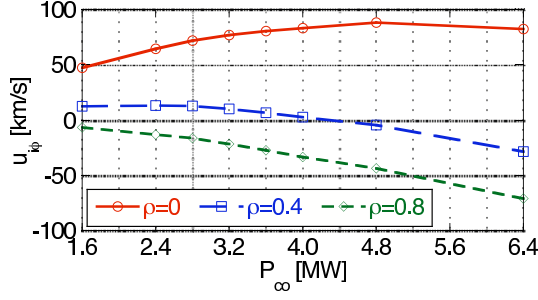
Fig. 2 Dependence of the toroidal rotation velocity $u_{i\phi}$ on the co-NBI input power P_{co} at $\rho = 0.0$, 0.4 and 0.8 in the case without FSTs. $P_{co} = 3.2\,\text{MW}$ in the reference case. Positive sign corresponds to the co-direction.

Fig. 3 Dependence of the toroidal rotation velocity $u_{i\phi}$ on the co-NBI input power P_{co} at $\rho = 0.0$, 0.4 and 0.8 in the case with FSTs.

cosities and thermal diffusivities are given and fixed at the values so that in a quasi-steady state the densities and the temperatures in simulations are similar to those in experiments. A calculation is carried out for 2 s where a plasma is assumed to reach a quasi-steady state.

Keeping the line-averaged density fixed at the value in the reference case by controlling a gas puff rate, we vary the input power of the co-tangential NBIs P_{co} from 1.6 MW to 6.4 MW, exceeding the maximum power $P_{co} \lesssim 3.5\,\text{MW}$ in the present JT-60U. Figure 2 shows that as the co-NBI power increases, the counter rotation near the periphery ($\rho = 0.8$, ρ is the normalized radius) becomes larger and the rotation at $\rho = 0.4$ changes the direction from co to counter because the $j \times B$ torque oriented to the counter direction becomes stronger. On the other hand, the on-axis co-rotation ($\rho = 0.0$) increases due to an increase in the direct collisional torque oriented to the co-direction. However, the on-axis co-rotation culminates in the maximum velocity of $\sim 90\,\text{km/s}$ at $P_{co} = 4.8\,\text{MW}$. Above 4.8 MW, the strong $j \times B$ torque near the periphery propagates to the core of the plasma through the perpendicular viscosity and to overcome the direct collisional torque especially near the magnetic axis, and then the co-rotation starts to decrease.

We found in Fig. 2 that the increase in the co-NBI power seems to relate to the enhancement of fast-ion losses due to ripple. Since equilibria remain unchanged during simulations, both the convective velocity and the diffusivity due to ripple and the area of the ripple well region are insensitive to the increase in the power, and therefore the characteristics of the ripple transport never change. On the other hand, the beam density increases with increasing the power. As is seen in Eq. (2), this increase may in turn promote the supply of the ripple-trapped beam ions through collisional deflection. The deflection rate ν_D is almost insensitive to the power because the beam velocity v_b is much faster than the ion thermal velocity v_{ti} even if the ion temperature increases with increasing the power. The diffusive process governing the loss of the banan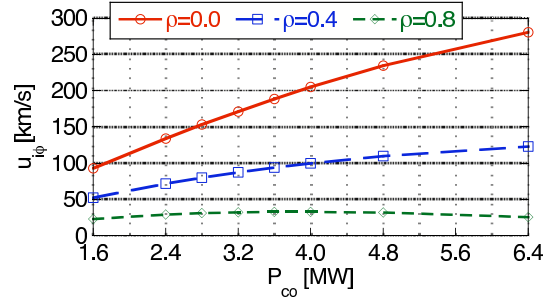a ions is much slower than the convective process mainly governing that of the ripple-trapped beam ions and ν_D/δ is very large. Therefore, as the power increases, the ripple-untrapped ions tend to accumulate in the plasma and the loss of the ripple-trapped ones becomes almost equal to the supply of them. As the power increases, therefore, the increase in their loss increases the outward fast-ion current and the resultant inward return current makes the $j \times B$ torque stronger.

After the insertion of FSTs reducing the ripple amplitude almost by half, the co-rotations at both $\rho = 0.0$ and 0.4 monotonically increase with increasing the power, and that at $\rho = 0.8$ is found to be saturated and then gradually decreases as shown in Fig. 3. Due to the reduction in the ripple amplitude, simulations show that the ripple-induced loss of fast ions and then the generated inward return current are almost reduced by half. Unlike the previous case, in this case with FSTs the direct collisional torque exceeds the generated $j \times B$ torque across the whole profile except the periphery where the $j \times B$ torque is still dominant. The co-rotation increases as the power increases within the realistic power range, $P_{co} \lesssim 3.5\,\text{MW}$.

4. Mitigation of the ripple effect by gas puff

In the previous section, we found that the significant loss of the ripple-trapped beam ions plays a major role in inducing the counter rotation near the periphery. Under the condition that the energy and the power of NBIs are fixed at $P_{co} = 3.2\,\text{MW}$, we seek the way to reduce the counter rotation by utilizing an externally-controllable source. We note that in the cases with a large gas puff rate of $\Gamma_0 > 0.3 \times 10^{20}\,\text{m}^{-2}\text{s}^{-1}$, the plasma does not reach a quasi-steady state at 2 s and it is still in a transient phase.

Taking account of the fact that the first term of Eq. (2) is much greater than the second term, we should find the way to lessen the first term in order to reduce the supply of the ripple-trapped beam ions. One way to do so is to reduce ν_D, mainly proportional to the bulk ion density n_i, and another way is to reduce the ripple-untrapped beam ion density n_b. Decreasing a gas puff rate is an easy way to reduce n_i. On the other hand, in order to reduce n_b with the NB power fixed, we should facilitate the thermalization
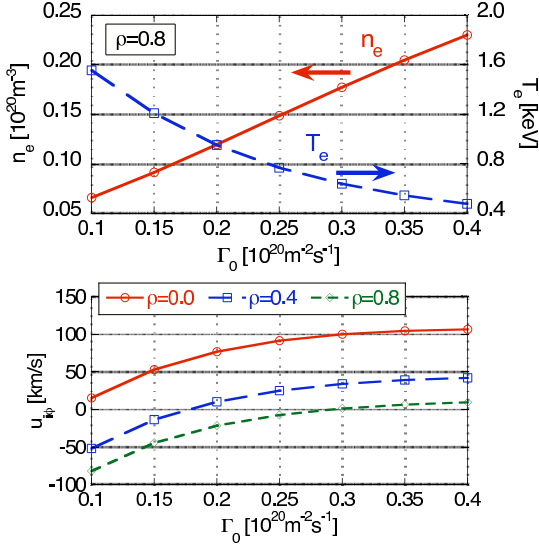
Fig. 4 Dependence of the electron density n_e (above), the electron temperature T_e (above) and the toroidal rotation velocity $u_{i\phi}$ (below) on the gas puff rate Γ_0 at $\rho = 0.0$, 0.4 and 0.8 in the case without FSTs. $P_{co} = 3.2\,\text{MW}$ and $\Gamma_0 = 0.2 \times 10^{20}\,\text{m}^{-2}\text{s}^{-1}$ in the reference case.

Fig. 5 Dependence of the toroidal rotation velocity $u_{i\phi}$ on the plasma current I_p at $\rho = 0.0$, 0.4 and 0.8 in the case without FSTs. $P_{co} = 3.2\,\text{MW}$ and $I_p = 1.0\,\text{MA}$ in the reference case.

of the beam ions by decreasing the energy slowing-down time τ_b. According to [7], τ_b is mainly proportional to τ_s, where τ_s denotes the ion-electron slowing-down time, and $\tau_s \propto T_e^{3/2}/n_e$, where n_e and T_e denote the electron density and temperature respectively. Decreasing τ_b, therefore, we should increase n_e or decrease T_e. An increase in the gas puff rate produces much more neutrals, leading to an increase in n_e and a decrease in T_e.

As is clear from the above consideration, although the application of gas puff is common to both two ways, one way cannot be coexistent with the other. By carrying out simulations, we then have to examine which effect is dominant when varying the gas puff rate Γ_0 from $0.1 \times 10^{20}\,\text{m}^{-2}\text{s}^{-1}$ to $0.4 \times 10^{20}\,\text{m}^{-2}\text{s}^{-1}$. As shown in Fig. 4, with increasing the gas puff rate the $j \times B$ torque weakens and the plasma tends to rotate in the co-direction. The amount of $\Gamma_0 = 0.3 \times 10^{20}\,\text{m}^{-2}\text{s}^{-1}$, 1.5 times as large as the reference case, is enough to vanish the counter rotation across the plasma.

We have found from the simulations that ν_D does not play an important role in the effect of gas puff on the ripple transport although it increases with increasing the density. In terms of the magnitude of ν_D/δ, regardless of the gas puff rate, it is still significantly large compared with other time-scales because of the smallness of the ripple amplitude δ. Then the magnitude of the ripple-untrapped density is found to play an essential role in the supply of the ripple-trapped density as seen in Eq. (2).

This result shows that the decrease in n_b and the increase in n_e and n_i due to the decrease in τ_b by gas puff cause a reduction in the supply of the ripple-trapped beam ions. This reduces the convective loss of beam ions and
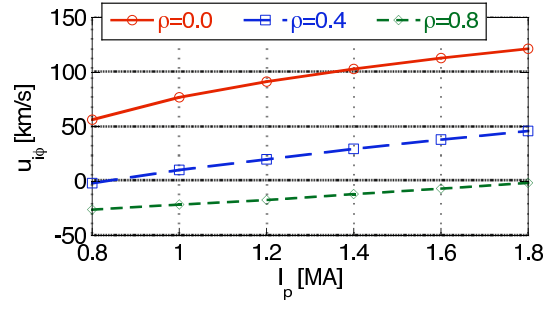
then the $j \times B$ torque. Furthermore, the reduction in the number of the beam ions leads to that in the diffusive loss of the banana ions, and this also contributes to this phenomenon. Here note that the decrease in the collisional slowing-down time between beam ions and electrons makes it easier to transfer the momentum from beam ions to electrons, and therefore the rotation of the beam ions slows down with increasing the gas puff rate. The deceleration of the fast-ion rotation reduces the driving force of the bulk-ion rotation oriented to the co-direction. This is the reason that the increase in the toroidal rotation velocity seems to be saturated at a certain level of the gas puff rate.

5. Dependence on the plasma current

The effect of the plasma current I_p on characteristics of the rotation associated with the ripple transport of fast ions seems to be complicated rather than that of the two actuators shown in the previous sections, because a change in the current leads to a change in the safety factor, affecting not only the ripple transport but also general characteristics of transport in the bulk plasma. It is therefore necessary to carry out self-consistent transport simulations to study the effect of the plasma current on the toroidal rotation associated with the ripple transport. We vary the current from 0.8 MA to 1.8 MA keeping the line-averaged bulk density fixed by gas puff. These upper and lower limits almost correspond to those in JT-60U with $B_\phi = 2.6\,\text{T}$. We note that we keep the transport coefficients in the bulk plasma throughout this study and we neglect the effect of the plasma current on them.

Before studying the dependence of the toroidal rotation on the plasma current, we have already confirmed from simulations without the effect of the ripple transport that the toroidal rotation does not correlate with the plasma current. Under the influence of the TF ripple, however, the simulations reveal the tendency in Fig. 5 that the co-rotation increases as the plasma current I_p increases. This implies that the plasma current affects the fast-ion losses caused by ripple. One of the important parameters for the ripple transport is the safety factor q [3]. If the toroidal

magnetic field remains unchanged, we keep in mind that the safety factor is inversely proportional to the plasma current, $q \propto I_\mathrm{p}^{-1}$.

We consider the cases with large I_p in the following. From Eq. (1), we can easily see that the ripple-trapped region where $\alpha < 1$ shrinks as I_p increases because α increases with decreasing q, leading to the reduction in the convective loss of fast ions. Similarly, the radial convective velocity arising from the vertical ∇B drift decreases because it is proportional to q in our model [3]. As shown in [6], $\delta_\mathrm{GWB} \propto q^{-3/2}$; hence the region with $\delta > \delta_\mathrm{GWB}$ where the stochastic diffusion is dominant shrinks as I_p increases, and then the diffusive loss of fast ions is reduced. Furthermore, the diffusion coefficient itself also decreases in conjunction with q. As a result, it is found that all these contributions tend to reduce the ripple transport when I_p increases.

With the increase in I_p, the reduction in the ripple transport decreases the return ion current flowing inward in the bulk plasma and at the same time the poloidal magnetic field B_θ increases. Since the $j \times B$ torque is expressed by the product of the radial current and B_θ, these two trends tend to offset their contributions to the torque. From the simulations, however, the dependence of B_θ on I_p is not the same as that of the ripple-induced radial current, and then the magnitude of the torque is not constant on I_p

Unlike the previous two actuators, the change in the current widely and significantly affects the characteristics of the plasma such as the current density, the toroidal electric field, the neoclassical viscosity, the radial electric field and the poloidal rotation. We should note that the toroidal rotation under the influence of fast-ion losses due to ripple is therefore determined not only by the direct effect of the change in I_p on the ripple transport but also by the balance among all the other effects induced by the change in I_p, implying the importance of a self-consistent analysis.

6. Conclusions and discussion

We have studied the dependence of the toroidal rotation on the NBI power, the gas puff rate and the plasma current by using the multi-fluid transport code TASK/TX [4] with the ripple transport model on the basis of the JT-60U-like parameters. The code has succeeded in qualitatively reproducing the rotation profiles in JT-60U under the influence of fast-ion losses due to ripple [3].

In the case without FSTs, i.e. a larger ripple amplitude than the present JT-60U with FSTs, the $j \times B$ torque oriented in the counter direction becomes stronger when we increase the power from co-tangential NBIs. We have found that this is due to the enhancement of the supply to the ripple-trapped beam ions with the increase in the power. On the contrary, the co-rotation increases as the power increases in the case with FSTs. By increasing the gas puff rate, we can mitigate the counter torque induced by the large loss of fast-ions due to ripple. The genera-

tion of the bulk ions through ionization near the periphery makes the collisions between beam ions and the bulk plasma frequent and thus raises the slowing-down rate. The increase in the slowing-down rate decreases the number of both the ripple-untrapped and ripple-trapped beam ions, and then their convective and diffusive losses are reduced, leading to the decrease in the counter $j \times B$ torque. We have also found that the co-rotation is enhanced as the plasma current increases. The increase in the current mitigates the ripple transport mainly through the decrease in the safety factor. However the mechanism is rather complicated because the other important plasma parameters such as the radial electric field and the neoclassical viscosity are simultaneously changed together with the current. This implies that the self-consistent treatment of all the variables is essential to this study.

In this paper we have focused on the characteristics of the toroidal rotation driven by co-NBI on the assumption that turbulent transport coefficients are given and fixed. JT-60U experiments have shown similar tendencies which we have obtained from the simulations in this paper: the direction of the rotation changes from counter to co as the gas puff rate increases, and the co-rotation increases as the plasma current increases. Especially in the latter case, however, it is mainly ascribed to the change in turbulent transport characteristics owing to the change in the plasma current, while we have fixed the turbulent transport coefficients in this study. Analyzing the toroidal rotation in experiments quantitatively, we have to carry out a more self-consistent simulation with a turbulent transport model, and then we should carefully examine the impact of the transport model on the toroidal rotation in the next study.

Unlike well-confined particles generated by co-NBIs, a part of banana particles generated by counter-NBIs is lost during a first bounce orbit because their trajectory intersects a wall. When we study characteristics of the toroidal rotation driven by counter-NBIs, the above-mentioned mechanism should be taken into account, which also induces a torque in the counter direction. Cooperation between the TASK/TX code and an orbit-following Monte Carlo code will be required.

Acknowledgements

[1] M. Yoshida *et al.*, Plasma Phys. Control. Fusion **48** 1673 (2006)
[2] P.C. de Vries *et al.*, Nucl. Fusion **48** 035007 (2008)
[3] M. Honda *et al.*, Nucl. Fusion **48** 085003 (2008)
[4] M. Honda and A. Fukuyama, J. Comp. Phys. **227** 2808 (2008)
[5] O.A. Anderson and H.P. Furth, Nucl. Fusion **12** 207 (1972)
[6] R.J. Goldston, R.B. White and A.H. Boozer, Phys. Rev. Lett. **47** 647 (1981)
[7] T.H. Stix, Plasma Phys. **14** 367 (1972)